



Contents

- 1 Abstract
- 1 Introduction
- 2 Study sites
- 3 Methods and materials
- 4 Results
- 4 Acknowledgments
- 5 References

Keywords

International Ocean Discovery Program, IODP, JOIDES Resolution, Expedition 362, Sumatra Seismogenic Zone, Sumatra Subduction Zone, Site U1480, Site U1481, outer-trench sediment, interstitial water, iodine

References (RIS)

MS 362-206

Received 19 December 2021

Accepted 21 April 2022

Published 30 June 2022

Data report: iodine in interstitial waters of outer-trench sediments off Sumatra Subduction Zone, IODP Expedition 362¹

S. Owari² and Hitoshi Tomaru³

¹Owari, S., and Tomaru, H., 2022. Data report: iodine in interstitial waters of outer-trench sediments off Sumatra Subduction Zone, IODP Expedition 362. In McNeill, L.C., Dugan, B., Petronotis, K.E., and the Expedition 362 Scientists, Sumatra Subduction Zone. *Proceedings of the International Ocean Discovery Program*, 362: College Station, TX (International Ocean Discovery Program). <https://doi.org/10.14379/iodp.proc.362.206.2022>

²School of Marine Resources and Environment, Tokyo University of Marine Science and Technology, Japan. Correspondence author: sowari0@kaiyodai.ac.jp

³Department of Earth Sciences, Chiba University, Japan.

Abstract

Outer-trench sediments offshore Sumatra were drilled at Sites U1480 and U1481 during International Ocean Discovery Program (IODP) Expedition 362. This expedition aimed to drill the thick outer-trench sediments (up to 4–5 km) to better understand the mechanisms of shallow megathrust slip in the Sumatra subduction system.

The iodine concentration dissolved in the interstitial water collected from these sites, ~250 km southwest of the subduction zone, was determined to understand the geochemical environment and iodine origin in the outer-trench sediment. The iodine concentrations increase with depth from seawater level to ~100 μM (270 times higher than seawater). In the outer-trench sediments offshore Sumatra, the iodine profile results from a complex process of the iodine-rich fluid derived from the basement, in situ iodine release caused by the decomposition of organic materials, and freshening due to mineral dehydration.

1. Introduction

Vertebrates and plankton absorb and concentrate iodine from seawater in the marine environment because of their biophilic nature. As their dead bodies sink to the seafloor and decompose as organic materials, the iodine taken up by their bodies is released from the sediment to the interstitial water (Pedersen and Price, 1980; Price et al., 1970). The iodine is enriched in the marine sediment and interstitial water hundreds to thousands of times compared to seawater through this process. Bromine also has a weak biophilic nature and shows similar behavior to iodine (Pedersen and Price, 1980; Price et al., 1970).

Methane is produced from organic materials after the degradation, and it sometimes shows a close association with iodine. Therefore, iodine is versatile for tracing methane (i.e., Fehn et al., 2007; Lu et al., 2008; Tomaru et al., 2009). The high iodine concentration of the interstitial water is observed in the forearc regions with high methane flux such as the Nankai Trough and Peru Margin (Martin et al., 1993; Tomaru et al., 2007).

Iodine is also enriched in serpentinized clast and mud matrix (nonsedimentary rocks) collected from deep forearc systems, indicating that subduction systems may contribute to iodine enrichment, reservoir, and a significant recycling system on the Earth (Snyder et al., 2005). Contrary to the high iodine flux setting in the forearc systems, the behavior of iodine is poorly understood in

outer-trench environments where the iodine concentration is relatively low. However, the abyssal sediment is one of the largest iodine budgets on the Earth's surface (Muramatsu and Wedepohl, 1998). Here we report on the analytical results of total iodine (I), bromine (Br), chlorine (Cl), and methane (CH₄) in pore waters collected at Sites U1480 and U1481 during Expedition 362 from the outer trench of the northwest Sumatra subduction zone.

2. Study sites

During Expedition 362, two sites were drilled on the Indian oceanic plate ~250 km southwest of the subduction zone to understand the role of thick sedimentary input section for shallow seismogenic slip (McNeill et al., 2016) (Figure F1A). The Sumatra-Andaman margin was formed by the subduction of the Indo-Australian oceanic plates under the Burma-Sunda plates and extended parallel to the western coast of Sumatra Island. Two sites were located in the outer-trench region, Site U1580 at 3°2.0447'N, 91°36.3481'E and Site U1481 at 2°45.261'N, 91°45.5771'E (Figure F1A, F1B). The Sumatra-Andaman margin is characterized by a high accumulation rate reaching ~250–350 m/My of the Bengal-Nicobar fan system (McNeill et al., 2017a). Sedimentary succession develops ~1.5 km at the research area and 4–5 km at the deformation front in the maximum (McNeill et al., 2016). The whole sedimentary succession at Site U1480 reaches 1431 meters below seafloor (mbsf) (McNeill et al., 2017a). Recovered sediments were mainly part of the Nicobar fan sediment and hemipelagic/pelagic sediment (Figures F1B, F2A). The fan sediment developed to be ~1250 m thick, and its accumulation started at 9.5 Ma (McNeill et al., 2017c; Backman et al., 2019). The Nicobar Fan deposits at Site U1481 are ~100 m thicker than those at Site U1480. The bottom of the Nicobar Fan deposits at 1250 mbsf at Site U1480 correlate to the sediment at 1350 mbsf at Site U1481 (McNeill et al., 2017c). The horizon of the bottom of Nicobar Fan deposits develops into a high-amplitude negative-polarity seismic reflector near the trench, which has been interpreted as a weak, porous, and high pore-fluid content layer (Dean et al., 2010) (Figure F1B).

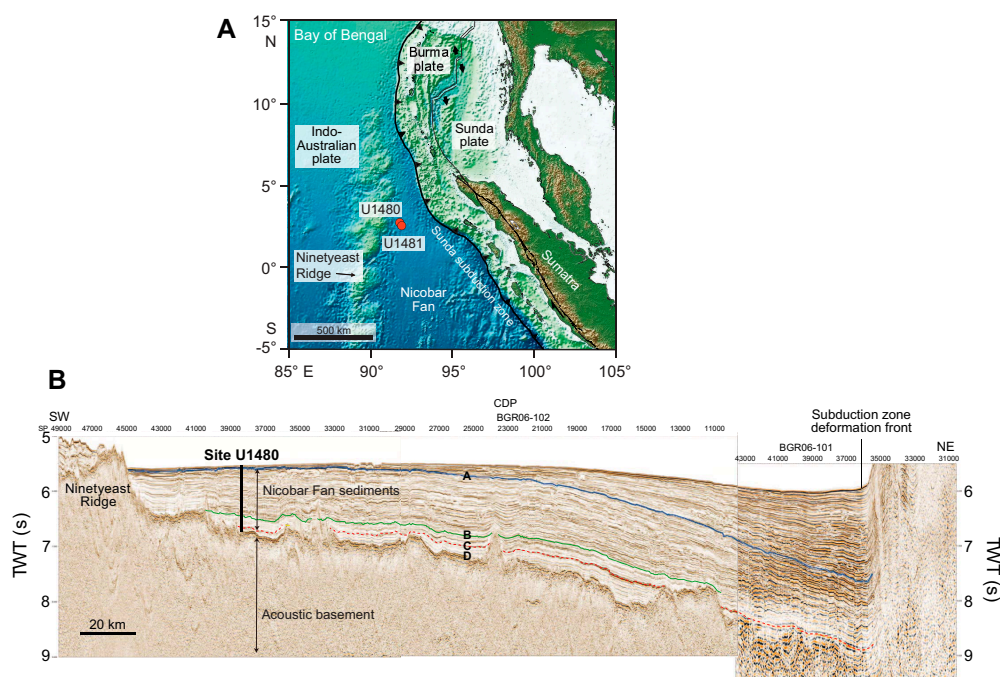


Figure F1. A. Tectonic setting of the Sumatran subduction zone showing plate boundary, Sites U1480 and U1481 (modified from Hüpers et al., 2017). B. Seismic profiles across the Indian oceanic plate west of the Sunda subduction zone, North Sumatra, from the Ninetyeast Ridge to the deformation front, including Site U1480. Seismic horizons A–D show lithologic unit boundaries. Seismic Horizon A (blue line) is the unconformable boundary between the trench wedge and the top of the Nicobar fan sediments. Seismic Horizon B (green line) is the transition from reflective to less reflective stratigraphy. Seismic Horizon C (dashed red line) is the high-amplitude reflector having negative polarity toward the subduction zone (Dean et al., 2010). Seismic Horizon D is an oceanic basement (Dugan et al., 2017). TWT = two-way travelttime, CDP = common depth point.

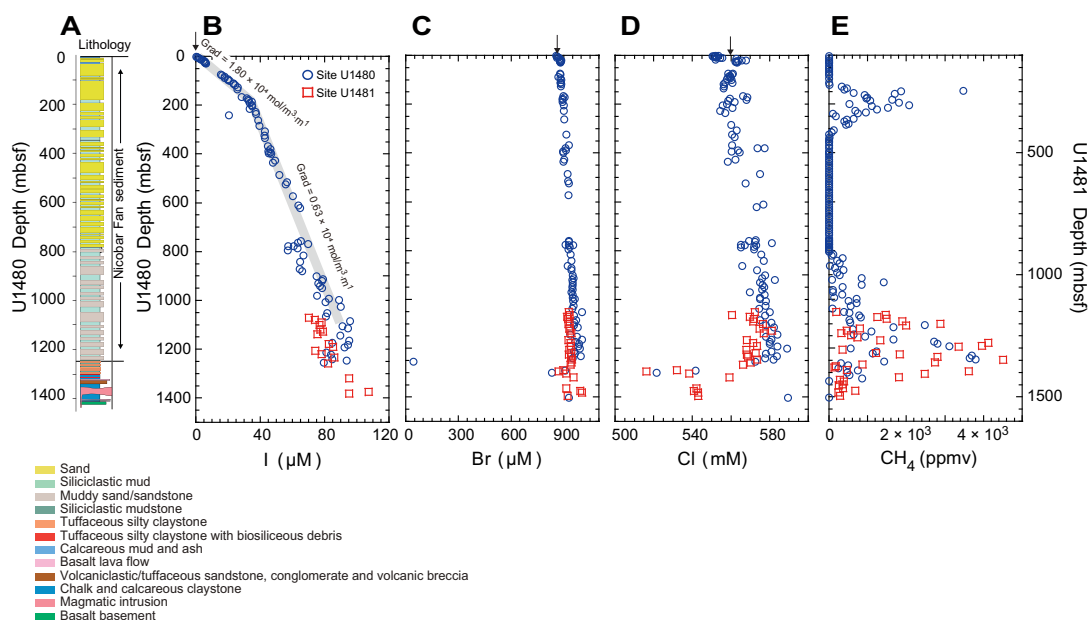


Figure F2. A. Lithology, Site U1480 (modified from Dugan et al., 2017). B–E. Depth profiles of (B) iodine, (C) bromine, (D) chlorine, and (E) methane concentration measured in interstitial water from Sites U1480 and U1481. Black arrows = standard seawater values (iodine = 0.4 μM ; bromine = 860 μM ; chlorine = 559 mM).

This horizon corresponds to the rapid decrease in chlorine concentration of the interstitial water, and this freshened water was due to the mineral dehydration caused by the pressure and temperature effects (Hüpers et al., 2017) (Figure F2D).

3. Methods and materials

Sediment cores were recovered from 0 to 1415 mbsf at Site U1480 and from 1172 to 1482 mbsf at Site U1481 (McNeill et al., 2017c). Sediment samples (10–25 cm) were collected on the catwalk at 2–4 samples per core (~10 m) immediately after core recovery. The inner part of the sediment, free from potential contamination of seawater and drilling mud, was then placed in the titanium squeezer, and the interstitial water was squeezed out through a 0.45 μm filter at a maximum pressure of 24.5 MPa using a hydraulic squeezer (CARVER, Model 3853-0 on the R/V *JOIDES Resolution*) (McNeill et al., 2017b).

Residual interstitial waters after onboard chemical analyses were transported to Japan. To determine the concentration of total iodine, interstitial waters were diluted by a factor of 2000 with deionized water (18 M Ω), and the following solution was added to the diluted sample: 0.75% tetramethylammonium hydroxide, 0.05% sodium sulfite, and 5 ppb cesium solution as an internal standard. The total iodine concentrations were measured by inductively coupled plasma–mass spectrometry (ICP-MS) (Agilent, 7500A) using argon carrier gas at the Micro Analysis Laboratory, Tandem accelerator (MALT), the University of Tokyo. The analytical precision of iodine was better than 0.15%.

The concentrations of total bromine and methane were determined on board along with standard shipboard analyses (McNeill et al., 2017b). To determine the concentration of total bromine, interstitial water was diluted by a factor of 100 with deionized water (18 M Ω). The total bromine concentration was measured by ion chromatography (Metrohm 850 Professional IC) using the eluant of 3.2 mM sodium carbonate and 1.0 mM sodium hydrogen carbonate with analytical precisions better than 2%.

The methane concentration was determined by gas chromatography (Agilent/HP 6890 Series II GC [GC3]) using helium as a carrier gas. The analytical precision of methane was better than 3%.

4. Results

All the halogen concentrations (iodine, bromine, and chlorine) at Sites U1480 and U1481 generally increase with depth from the seafloor to right above the basement except for a freshening depth at 1250 mbsf (Figure F2B, F2C, F2D): iodine to ~100 μM , bromine to 860 μM , and chlorine to ~590 μM . McNeill et al. (2017c) and Dugan et al. (2017) pointed to the input of altered seawater enriched in chlorine and sulfate derived from the basement. Our results indicate that this fluid is significantly enriched in iodine compared to other halogens. Organic-rich sediment resulting from high biological productivity on the continental margin and active decomposition of organic materials due to increasing temperature associated with subduction contribute to iodine enrichment in interstitial water (Lu et al., 2008; Morris, 1987; Tomaru et al., 2007). Therefore, iodine-rich fluid at the drilling sites is likely to be transported from forearc sediment to outer-trench sediment through the basement.

The positive peaks of methane concentration at 200 and 1250 mbsf indicate that iodine is released from the organic materials into the interstitial water together with methane after decomposition at these depths (Figure F2E). The gradient of iodine concentration at Site U1480 changes at 200 mbsf: $1.80 \times 10^4 \text{ mol/m}^3/\text{m}$ from 0 to 200 mbsf and $0.63 \times 10^4 \text{ mol/m}^3/\text{m}$ from 200 to 1100 mbsf. The diffusive iodine flux is calculated by Fick's first law from the linear part of the gradient (Figure F2B). The diffusive flux of iodine in the sediment (J_{sed}) is calculated as

$$J_{\text{sed}} = -\Phi \cdot D_{\text{sed}} \cdot \frac{\delta C}{\delta x}, \quad (1)$$

where Φ is the sediment porosity, D_{sed} is the diffusion coefficient for iodine in sediments, and $\delta C/\delta x$ is the concentration gradient. The diffusion coefficient in the sediments (D_{sed}) and tortuosity (θ^2) are calculated using the following equations:

$$D_{\text{sed}} = \frac{D^{\text{SW}}}{\theta^2}, \text{ and} \quad (2)$$

$$\theta^2 = 1 - \ln(\Phi^2), \quad (3)$$

where D^{SW} is the diffusion coefficient for iodine in seawater (Schulz and Zabel, 2006). The iodine flux at Site U1480 is $-1.31 \times 10^{-6} \text{ mol/m}^2/\text{y}$ from 0 to 200 mbsf and $-1.13 \times 10^{-9} \text{ mol/m}^2/\text{y}$ from 200 to 1100 mbsf. The iodine flux in outer-trench sediment is 13–80 times smaller than the iodine flux in forearc sediment at the Nankai Trough and Peru Margin (Fehn et al., 2007; Muramatsu et al., 2007; Tomaru and Fehn, 2015). The decrease of iodine flux at 200 mbsf indicates that the in situ iodine release may contribute to the higher iodine flux between 0 and 200 mbsf. Iodine concentration between 1200 and 1250 mbsf shows a slight decrease, whereas iodine would increase due to the iodine release from in situ sediment at ~1250 mbsf. This is probably because the freshening effect of interstitial water caused by the mineral dehydration is more significant than the in situ iodine release at 1250 mbsf (Figure F2B, F2D) (Hüpers et al., 2017). Despite the freshening on chlorine and bromine (Figure F2C, F2D), the decrease of iodine concentration is relatively small, indicating chlorine and bromine are released in smaller amounts during organic decomposition than iodine (Martin et al., 1993). In summary, the concentration of iodine of the outer-trench sediment offshore Sumatra reflects iodine-rich fluid derived from the basement and near the basement, in situ iodine release caused by the decomposition of organic materials at 200 mbsf, and freshening due to mineral dehydration at 1250 mbsf.

5. Acknowledgments

This research used samples and data provided by the International Ocean Discovery Program (IODP). We thank the onboard technicians, Siem Offshore officers and crew, the drilling crew, and the science party of IODP Expedition 362. We are also grateful to the Micro Analysis Laboratory, Tandem accelerator (MALT), the University of Tokyo, for the iodine analysis. This work was supported by the Research Fellowship for Young Scientists from the Japan Society for the Promotion

of Science (JSPS) [grant number 16J02710] and IODP Expedition 362 After Cruise Research Program, Japan Agency for Marine-Earth Science and Technology (JAMSTEC).

References

- Backman, J., Wenchuang, C., Kachovich, S., Mitchison, F.L., Petronotis, K.E., Tao, Y., and Zhao, X., 2019. Data report: revised age models for IODP Sites U1480 and U1481, Expedition 362. In McNeill, L.C., Dugan, B., Petronotis, K.E., and the Expedition 362 Scientists, Sumatra Subduction Zone. *Proceedings of the International Ocean Discovery Program*, 362: College Station, TX (International Ocean Discovery Program).
<https://doi.org/10.14379/iodp.proc.362.202.2019>
- Dean, S.M., McNeill, L.C., Henstock, T.J., Bull, J.M., Gulick, S.P.S., Austin, J.A., Bangs, N.L.B., Djajadihardja, Y.S., and Permana, H., 2010. Contrasting décollement and prism properties over the Sumatra 2004–005 earthquake rupture boundary. *Science*, 329(5988):207–210. <https://doi.org/10.1126/science.1189373>
- Dugan, B., McNeill, L., Petronotis, K., and the Expedition 362 Scientists, 2017. Expedition 362 Preliminary Report: Sumatra Subduction Zone: International Ocean Discovery Program <https://doi.org/10.14379/iodp.pr.362.2017>
- Fehn, U., Snyder, G.T., and Muramatsu, Y., 2007. Iodine as a tracer of organic material: ¹²⁹I results from gas hydrate systems and fore arc fluids. *Journal of Geochemical Exploration*, 95(1–3):66–80.
<https://doi.org/10.1016/j.gexplo.2007.05.005>
- Hüpers, A., Torres, M.E., Owari, S., McNeill, L.C., Dugan, B., Henstock, T.J., Milliken, K.L., Petronotis, K.E., Backman, J., Bourlange, S., Chemale, F., Chen, W., Colson, T.A., Frederik, M.C.G., Guèrin, G., Hamahashi, M., House, B.M., Jeppson, T.N., Kachovich, S., Kenigsberg, A.R., Kuranaga, M., Kutterolf, S., Mitchison, F.L., Mukoyoshi, H., Nair, N., Pickering, K.T., Pouderoux, H.F.A., Shan, Y., Song, I., Vannucchi, P., Vrolijk, P.J., Yang, T., and Zhao, X., 2017. Release of mineral-bound water prior to subduction tied to shallow seismogenic slip off Sumatra. *Science*, 356(6340):841–844. <https://doi.org/10.1126/science.aal3429>
- Lu, Z., Tomaru, H., and Fehn, U., 2008. Iodine ages of pore waters at Hydrate Ridge (ODP Leg 204), Cascadia margin: implications for sources of methane in gas hydrates. *Earth and Planetary Science Letters*, 267(3–4):654–665.
<https://doi.org/10.1016/j.epsl.2007.12.015>
- Martin, J.B., Gieskes, J.M., Torres, M., and Kastner, M., 1993. Bromine and iodine in Peru margin sediments and pore fluids: implications for fluid origins. *Geochimica et Cosmochimica Acta*, 57(18):4377–4389.
[https://doi.org/10.1016/0016-7037\(93\)90489-J](https://doi.org/10.1016/0016-7037(93)90489-J)
- McNeill, L.C., Dugan, B., Backman, J., Pickering, K.T., Pouderoux, H.F.A., Henstock, T.J., Petronotis, K.E., Carter, A., Chemale, F., Milliken, K.L., Kutterolf, S., Mukoyoshi, H., Chen, W., Kachovich, S., Mitchison, F.L., Bourlange, S., Colson, T.A., Frederik, M.C.G., Guèrin, G., Hamahashi, M., House, B.M., Hüpers, A., Jeppson, T.N., Kenigsberg, A.R., Kuranaga, M., Nair, N., Owari, S., Shan, Y., Song, I., Torres, M.E., Vannucchi, P., Vrolijk, P.J., Yang, T., Zhao, X., and Thomas, E., 2017a. Understanding Himalayan erosion and the significance of the Nicobar Fan. *Earth and Planetary Science Letters*, 475:134–142. <https://doi.org/10.1016/j.epsl.2017.07.019>
- McNeill, L.C., Dugan, B., Petronotis, K.E., Backman, J., Bourlange, S., Chemale, F., Jr., Wenhuan, C., Colson, T.A., Frederik, M.C.G., Guèrin, G., Hamahashi, M., Henstock, T., House, B.M., Hüpers, A., Jeppson, T.N., Kachovich, S., Kenigsberg, A.R., Kuranaga, M., Kutterolf, S., Milliken, K.L., Mitchison, F.L., Mukoyoshi, H., Nair, N., Owari, S., Pickering, K.T., Pouderoux, H.F.A., Yehua, S., Song, I., Torres, M.E., Vannucchi, P., Vrolijk, P.J., Tao, Y., and Zhao, X., 2017b. Expedition 362 methods. In McNeill, L.C., Dugan, B., Petronotis, K.E., and the Expedition 362 Scientists, Sumatra Subduction Zone. *Proceedings of the International Ocean Discovery Program*, 362: College Station, TX (International Ocean Discovery Program). <https://doi.org/10.14379/iodp.proc.362.102.2017>
- McNeill, L.C., Dugan, B., Petronotis, K.E., Backman, J., Bourlange, S., Chemale, F., Jr., Wenhuan, C., Colson, T.A., Frederik, M.C.G., Guèrin, G., Hamahashi, M., Henstock, T., House, B.M., Hüpers, A., Jeppson, T.N., Kachovich, S., Kenigsberg, A.R., Kuranaga, M., Kutterolf, S., Milliken, K.L., Mitchison, F.L., Mukoyoshi, H., Nair, N., Owari, S., Pickering, K.T., Pouderoux, H.F.A., Yehua, S., Song, I., Torres, M.E., Vannucchi, P., Vrolijk, P.J., Tao, Y., and Zhao, X., 2017c. Expedition 362 summary. In McNeill, L.C., Dugan, B., Petronotis, K.E., and the Expedition 362 Scientists, Sumatra Subduction Zone. *Proceedings of the International Ocean Discovery Program*, 362: College Station, TX (International Ocean Discovery Program). <https://doi.org/10.14379/iodp.proc.362.101.2017>
- McNeill, L.C., Dugan, B.E., and Petronotis, K.E., 2016. Expedition 362 Scientific Prospectus: The Sumatra Subduction Zone. International Ocean Discovery Program. <https://doi.org/10.14379/iodp.sp.362.2016>
- Morris, R.J., 1987. The formation of organic-rich deposits in two deep-water marine environments. In Brooks, J., and Fleet, A.J. (Eds.), *Marine Petroleum Source Rocks*. Geological Society Special Publication, 26:153–166.
<https://doi.org/10.1144/GSL.SP.1987.026.01.09>
- Muramatsu, Y., Doi, T., Tomaru, H., Fehn, U., Takeuchi, R., and Matsumoto, R., 2007. Halogen concentrations in pore waters and sediments of the Nankai Trough, Japan: implications for the origin of gas hydrates. *Applied Geochemistry*, 22(3):534–556. <https://doi.org/10.1016/j.apgeochem.2006.12.015>
- Muramatsu, Y., and Hans Wedepohl, K., 1998. The distribution of iodine in the earth's crust. *Chemical Geology*, 147(3–4):201–216. [https://doi.org/10.1016/S0009-2541\(98\)00013-8](https://doi.org/10.1016/S0009-2541(98)00013-8)
- Pedersen, F.D., and Price, N.B., 2019. The geochemistry of iodine and bromine in sediments of the Panama Basin. *Journal of Marine Research*, 38(3):397–411.
<https://images.peabody.yale.edu/publications/jmr/jmr38-03-02.pdf>
- Price, N.B., Calvert, S.E., and Jones, P.G.W., 1970. Distribution of iodine and bromine in the sediments of the southwestern Barents Sea. *Journal of Marine Research*, 28:22–34.
<https://images.peabody.yale.edu/publications/jmr/jmr28-01-03.pdf>

- Schulz, H.D., and Zabel, M. (Eds.), 2006. *Marine Geochemistry*: Berlin (Springer).
<https://doi.org/10.1007/3-540-32144-6>
- Snyder, G.T., Savov, I.P., and Muramatsu, Y., 2005. Iodine and boron in Mariana serpentinite mud volcanoes (ODP Legs 125 and 195): implications for forearc processes and subduction recycling. In Shinohara, M., Salisbury, M.H., and Richter, C. (Eds.), *Proceedings of the Ocean Drilling Program, Scientific Results, 195*: College Station, TX (Ocean Drilling Program). <https://doi.org/10.2973/odp.proc.sr.195.102.2005>
- Tomaru, H., and Fehn, U., 2015. Movement of fluids in the Nankai Trough area: insights from ¹²⁹I and halogen distributions along the IODP NanTroSEIZE transect. *Geochimica et Cosmochimica Acta*, 149:64–78.
<https://doi.org/10.1016/j.gca.2014.10.028>
- Tomaru, H., Fehn, U., Lu, Z., Takeuchi, R., Inagaki, F., Imachi, H., Kotani, R., Matsumoto, R., and Aoike, K., 2009. Dating of dissolved iodine in pore waters from the gas hydrate occurrence offshore Shimokita Peninsula, Japan: ¹²⁹I results from the D/V Chikyu shakedown cruise. *Resource Geology*, 59(4):359–373.
<https://doi.org/10.1111/j.1751-3928.2009.00103.x>
- Tomaru, H., Lu, Z., Fehn, U., Muramatsu, Y., and Matsumoto, R., 2007. Age variation of pore water iodine in the eastern Nankai Trough, Japan: evidence for different methane sources in a large gas hydrate field. *Geology*, 35(11):1015–1018. <https://doi.org/10.1130/G24198A.1>